

Unveiling the Power of Negative Ion Mode ESI-MS: Identifying Species with Remarkable Signal Intensity and Collisional Stability

Benjamin B. Warnes,[‡] Jasmine Chihabi,[‡] and Jeffrey M. Manthorpe*

Department of Chemistry, Carleton University, Ottawa, Ontario K1S 5B6, Canada

ABSTRACT: Electrospray ionization mass spectrometry has long been the standard and most prevalent ionization method in mass spectrometry to detect and analyze molecules of low volatility that are relevant biologically, environmentally, and industrially. However, only a small number of analyses are conducted in negative ion mode, which has led to a dogmatic bias toward positive ion mode despite advantageous properties of the negative polarity, including lower background noise and divergent tandem mass spectrometry behavior. We hypothesized that this bias was rooted in the relatively poor ionization efficiency of anionic functional groups seen in biochemistry; to explore this notion herein we evaluated 25 ions based on three criteria: (1) signal intensity relative to a sodium dodecylsulfate internal standard; (2) resistance to collision induced dissociation based on survival of the precursor ion; and (3) diagnostic tandem mass spectrometry behavior. Among these species, highly fluorinated ions exhibiting weakly coordinating and hydrophobic properties contributed to enhanced signal intensities. Trifluoromethanesulfonyl-containing ions proved to be unexpectedly labile, while tetrakis[3,5-bis(trifluoromethyl)phenyl]borate anion (**23**) and bis(nonafluoro-1-butane)sulfonimidate (**25**) were determined to be of optimal signal intensity with signal intensity ratios relative to sodium dodecylsulfate (**12** + Na⁺) of 332.0% ± 25.0% and 939.0% ± 92.0%, respectively, as well as survival yields of 100.0% ± 0.0% and 72.6% ± 0.8% at -50 eV. To further emphasize their optimal signal intensity, ions tetrakis[3,5-bis(trifluoromethyl)phenyl]borate anion (**23**) and bis(nonafluoro-1-butane)sulfonimidate (**25**) were comparable in signal intensity across solvents of acetonitrile, methanol, isopropanol, water, and their respective 1:1 mixtures. Facile preparation of various salts of bis(nonafluoro-1-butane)sulfonimidate led to additional evaluation of cation effects where the signal intensity ratio ranged from 939.0% ± 92.0% to 3195.0% ± 145.0% across K⁺, NH₄⁺, Na⁺, and H⁺ counter cations. The dogma of negative ion mode being less sensitive was then challenged by the analysis of the signal intensity of ion **25** to tetra-*n*-butylammonium, tetra-*n*-butylphosphonium, and (4-methylphenyl)diphenylsulfonium cations. These experiments showed that **25** was more sensitive by between 136.2% ± 5.5% and 180.7% ± 13.8%, thereby successfully challenging the positive polarity bias.

Electrospray ionization mass spectrometry (ESI-MS) is an indispensable tool for the analysis of high mass-to-charge ratio (m/z) analytes. Its reliance on non-covalent interactions for the formation of a pseudomolecular ion dictates that a minimal residual energy is imparted to the analyte making the analysis of intact pseudomolecular ions possible.¹ Consequently, the non-destructive nature of ESI-MS has contributed to the far-reaching applications of the technique to biological^{2,3}, environmental⁴, food production⁵, and clinical settings⁶.

Ionization efficiency (IE), which represents the proportion of ions generated from an analyte of interest that are transmitted into the gas phase,⁷ is a crucial parameter in the ESI process and has a profound effect on sensitivity and detection. One of the most probed acidic functionalities contained within biomolecules (e.g., amino acids, fatty acids) are carboxylic acids.^{8,9} Unfortunately, these typically suffer from poor IEs in negative polarity ESI due to the high gas phase acidity parameter of these species.¹⁰ On the other hand, positive polarity thrives on an abundance of basic functionalities (e.g., amines, imidazoles) with higher IEs.¹¹ This has encouraged much of ESI based analyses of

biomolecules to be conducted in the positive polarity and has simultaneously created a longstanding¹² polarity bias wherein "it is well known that negative ion mode ESI-MS is generally less sensitive than the positive ion mode"¹³ due to inherent limitations such as corona discharge,¹⁴ salt clustering,¹⁵ and the requisite use of solvents that support the formation of excess negative charge.¹⁶

In 2017, Liigand et al. successfully compared the ionization efficiencies (IE) of both ESI polarities, revealing that the negative polarity is often more sensitive, boasting decreased background noise and increased signal-to-noise (S/N) ratios.¹⁴ It is worth noting that positive polarity ESI relies on associative mechanisms to form the pseudomolecular ion (i.e., neutral species (M) associates with a cation such as H⁺, Na⁺, or NH₄⁺). This has frequently resulted in signal splitting further increasing spectral complexity and decreasing signal strength. Conversely, while the negative ion mode can still give rise to associative mechanisms to form negatively charged adducts, this phenomenon is far more prevalent in positive ion mode.¹⁷ Therefore, anion formation in negative ion mode ESI-MS is typically reliant on dissociative mechanisms where M loses a cation, such as

proton, ammonium, or metal ion. Such dissociative formation of ions also means that signal splitting and the challenges associated with it are rarely encountered.

To address the aforementioned challenges encountered in positive polarity ESI, targeted chemical derivatization (CD) strategies involving the chemical transformation of a reactive functional group within an analyte have been developed. CD reagents are practically designed to alter analyte properties to benefit separation and detection by mass spectrometry (MS) through: (1) enhanced retention times of poorly retained analytes,^{18,19} (2) reduced background noise via increased m/z of the analyte, (3) improved structural information in fragmentation in tandem mass spectrometry (MS/MS),²⁰ and (4) quenching of potentially labile functional groups.

Fixed charge CD is of particular significance in the field since analytes lacking basic or acidic functional groups often suffer from low IE even after CD.²¹ The majority of these rely on positively charged ammonium, phosphonium, and sulfonium groups for fixed charge induction at a specific functional group.²² These have been designed to specifically target, *inter alia*, amine, carboxyl, and hydroxyl moieties within biological molecules including amino acids,^{23–25} phospholipids,^{26–28} steroids,^{29,30} fatty acids,^{27,31} and peptides.^{32–34} To date, these various studies have demonstrated significant improvements in chromatographic separations, charge state, and the S/N ratio leading to enhanced sensitivity.²² Furthermore, valuable structural information has been provided via charge remote fragmentation MS/MS experiments.^{35–37}

For these reasons, the field of fixed charge CD has received much attention and focus in recent years with several fixed positive charge CD reagents being preceded in the literature and commercially.²² In stark contrast, current advancements of CD reagents for ESI-MS have virtually overlooked the negative polarity with only a small number of examples emergent in the literature.^{38–40} It may be suggested that this state of affairs stems from the apparent dearth of analogous negatively charged functional groups that are commercially available and bench stable displaying adequate chemical stabilities in solution well as in MS experiment conditions. However, this predefined gap in fixed charge CD only strengthens the notion of an existing and persistent positive polarity bias.

It was our hypothesis that this pro-positive ion mode dogma originates not from the inherent properties of ESI, but in the relatively greater ionization efficiency of the commonly investigated (*i.e.*, largely biochemical) functional groups amenable to positive ion mode versus those species biased toward ionization in the negative polarity. Thus, herein, 25 different ions (Chart 1) featuring either highly acidic functionality or a permanent negative charge were evaluated to challenge the current dogma that the positive polarity is inherently more sensitive than the negative. The evaluation of these candidates was conducted based on three criteria: (1) signal intensity; (2) precursor ion stability to collision-induced dissociation (CID), and (3) diagnostic MS/MS behavior.

At the outset of this work, we sought to evaluate signal intensity differences between desired charged candidates by EMS scans of equimolar concentrations of the desired charged candidates and an internal standard of sodium dodecyl sulfate (SDS, **12** + Na⁺). Subsequent MS/MS behaviour and precursor ion stability was also probed through the calculated survival yield (SY): the percentage of a precursor ion that remains intact after CID by acquiring product ion scans at a constant collision energy. The optimal performing charged candidates were then evaluated in different solvent mixtures and cations present in the sample matrix. Subsequently, the dogma of the inferiority of the negative ion mode was addressed experimentally by comparison to species bearing a fixed permanent positive charge.

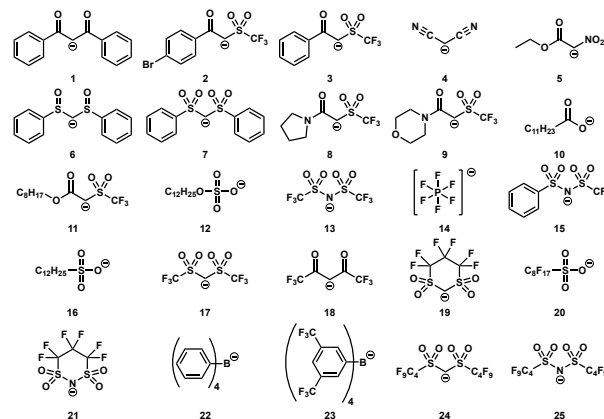


Chart 1. Ions evaluated in the negative polarity ESI relative to an internal standard (**12**)

Materials and Methods

Chemicals and Materials

Dibenzoylmethane (**1** + H⁺) was purchased from BDH Chemicals Ltd. (Poole, UK, England). Malononitrile (**4** + H⁺), lauric acid (**10** + H⁺), lithium bis((trifluoromethyl)sulfonyl)imide (**13** + Li⁺), ammonium hexafluorophosphate (**14** + NH₄⁺), sodium dodecylsulfonate (**16** + Na⁺), sodium tetraphenylborate (**22** + Na⁺), tetra-*n*-butylammonium bromide (**26** + Br⁻), tetra-*n*-butylphosphonium bromide (**27** + Br⁻), (4-methylphenyl)diphenylsulfonium triflate (**28** + TfO⁻), and tetraethylammonium perfluoro-1-octanesulfonate (**20** + Et₄N⁺) were purchased from Sigma Aldrich (St. Louis, MO, USA). Bis((trifluoromethyl)sulfonyl)methane (**17** + H⁺) was purchased from Synquest Laboratories (Alachua, FL, USA). Sodium dodecylsulfate (SDS, **12** + Na⁺) was purchased from Bio-Rad Laboratories (Canada) Ltd. (Mississauga, ON, Canada). Hexafluoroacetylacetone (**18** + H⁺) and ethyl nitroacetate (**5** + H⁺) were purchased from Tokyo Chemical Industry (TCI) (Portland, OR, USA).

Compounds (**2** + H⁺)⁴¹, (**3** + H⁺)⁴¹, (**6** + H⁺)⁴², (**7** + H⁺)⁴³, (**8** + H⁺)⁴⁴, (**9** + H⁺)⁴⁴, (**15** + Na⁺)⁴⁵, and (**24** + Na⁺)⁴⁶ were synthesized from their precursors based on literature procedures (see Supporting Information). Bis(nonafluorobutanesulfonyl)imide (**25** + H⁺) and potassium bis(nonafluoro-1-butanesulfonyl)imidate (**25** + K⁺) were purchased from Wako Chemicals (Osaka, OF, Japan), and (**25** +

H⁺) was used to synthesize (**25** + Na⁺) and (**25** + NH₄⁺) (see Supporting Information).

Perfluoro-1,3-dithiane 1,1,3,3-tetraoxide (**19** + H⁺) and perfluoro-1,3,2-dithiazine 1,1,3,3-tetraoxide (**21** + H⁺) were generously provided by Prof. Dr. Hikaru Yanai, Tokyo University of Pharmacy and Life Sciences (Tokyo, TO, Japan). Sodium tetrakis(3,5-bis(trifluoromethyl)phenyl)borate (**23** + Na⁺) was generously supplied by Prof. Dr. Charles McDonald, Dalhousie University (Halifax, NS, Canada).

Liquid chromatography mass spectrometry (LC-MS) grade acetonitrile, methanol, isopropanol, and water were purchased from Fisher Scientific (Rochester, NY, USA).

MS Sample Preparation

All samples were prepared by weighing out a prescribed amount of given material into an Agilent (Santa Clara, CA, USA) 2 mL screw top vial with a polytetrafluoroethylene (PTFE) coated screw cap. Then, 1 mL of LC-MS grade acetonitrile was added to the HPLC vial and vortexed for 30 s to ensure complete dissolution of the desired compound. This stock sample solution was then diluted to a concentration of 1 mM in the desired compound.

After preparation of a 1 mM stock solution in desired compound, a 10 μM solution of equimolar concentrations of the desired compound and SDS were made by serial dilution of the stock solution into a 2 mL HPLC vial. The resultant solution was vortexed for 30 s prior to further serial dilutions. Two more serial dilutions were conducted from the 10 μM standard solution of the desired compound and SDS in the same manner as above to concentrations of 2.5 μM and 0.5 μM.

MS Intensity Ratio Experiments

To determine the intensity ratios of desired compounds, 400 μL of the desired standard solution containing equimolar concentrations of the desired charged tag and SDS were loaded into a 1 mL gas tight Hamilton syringe (Hamilton Company, Reno, NV). The syringe was then added to a Harvard Apparatus 11Plus (Holliston, MA) syringe pump at a flow rate of 10 μLmin⁻¹. The syringe was connected via PEEK tubing to an AB Sciex 4000 QTRAP with a Turbo V ESI source (AB Sciex, Framingham, MA). EMS spectra were acquired in the negative ion mode with the following parameters: IS voltage: -4000 V; curtain gas: 20 psi; declustering potential: -30 eV; collision energy: -10 eV; collision gas: medium; source temperature: 50 °C.

For determination of the intensity ratios of the desired compounds to SDS, EMS scans were conducted for a standard duration of 0.379 min. The intensity ratio of the desired compound to SDS was then determined by dividing the maximum peak height of the desired compound by the maximum peak height of SDS. All intensity ratios were determined at a concentration of 0.5 μM in desired compound and SDS and were based on a triplicate dataset corresponding to the same equimolar standard solution.

MS Survival Yield Experiments

To acquire the SY of the desired compounds, the same 0.5 μM standard solution was utilized at the same concentration, sample loading, flow rate, and instrumentation as the intensity ratio experiments. Product ion scans were conducted using the following parameters: IS voltage: -4000 V; collision energy: -50 eV; curtain gas: 20 psi; declustering potential: -30 eV; collision gas: medium; source temperature: 50 °C. Precursor ions were selected based on the expected *m/z* of the desired compound. The sum of all the product ion scans over a duration of 110 scans for all the desired compounds analyzed were determined and was conducted in triplicate using the same 0.5 μM standard solution of desired compound and SDS.

The SY was determined by taking the intensity of the precursor ion and subsequently dividing the sum of the intensities of all product ions that are ≥2.5% of the base peak.

SY experiments at -20 eV and -30 eV were conducted in the same manner with all parameters remaining unchanged except for the collision energy. Calculations of SY at these collision energies were performed as previously mentioned above.

MS Cation Effect Experiments

To examine the effects of counter cations on signal intensity, solutions of (**25**+H⁺) and (**25**+K⁺) were prepared in an equimolar concentration to (**12** + Na⁺) at a concentration of 0.5 μM and the signal intensities were computed, respectively. To discern the effect of sodium and ammonium counter cations, solutions of (**25** + H⁺) were prepared with a 10 μL spike of saturated sodium bicarbonate and 28% aqueous ammonia at the same concentration of 0.5 μM.

Signal intensity MS experiments for (**25** + H⁺), (**25** + K⁺), (**25** + Na⁺), (**25** + NH₄⁺) were acquired in the negative ion mode with the exact parameters outlined in the signal intensity experiments.

MS Solvent Effects Experiments

To evaluate the effects of solvent on signal intensity, solutions containing a mixture of ions **18–25** were prepared at an equimolar concentration of 0.5 μM. The solvents that were probed in these experiments were acetonitrile, methanol, isopropanol, water, and their respective 1:1 solvent mixtures. MS experiments were then conducted with the same injection and instrumental parameters as utilized in the signal intensity ratio experiments. The signal intensity ratios relative to SDS were then computed for ions **18–25** for each solvent and solvent mixture.

MS Polarity Comparison Experiments

To discern the difference between the positive and negative modes, equimolar solutions of (**25** + K⁺) and (**26** + Br⁻), (**27** + Br⁻), and (**28** + TfO⁻) were prepared at a concentration of 0.5 μM.

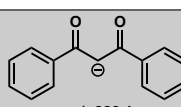
Negative ion mode ESI-MS experiments were conducted according to the same parameters outlined in the signal intensity ratio experiments. After each negative ion mode MS experiment, the electrospray was then stopped and was then switched to the positive polarity using the following instrument parameters: IS voltage: 4000 V; curtain gas: 20 psi; declustering potential: 30 eV; collision energy: 10 eV; collision gas: medium; source temperature: 50 °C. For each polarity switch, three replicate experiments were conducted at a duration of 0.379 min. In total, polarity was switched three times generating three sets of triplicate experiments. For each set of experiments, the signal intensity ratio of **25** to the signal intensities of **26**, **27**, and **28** were computed and averaged over three separate replicates.

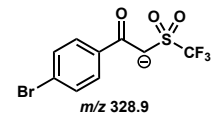
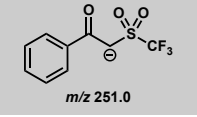
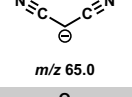
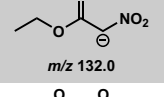
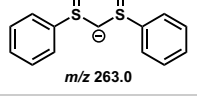
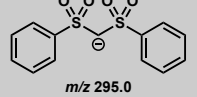
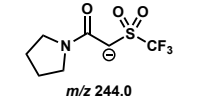
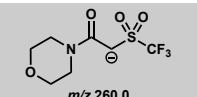
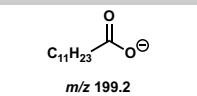
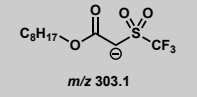
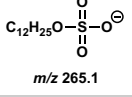
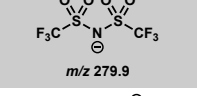
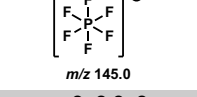
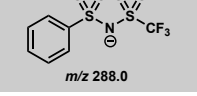
Results and Discussion

To evaluate the performance of each individual ion, the intensity ratios relative to an internal standard (SDS) were determined at an equimolar concentration. SDS was chosen as the internal standard to compare negatively charged ions based on its ubiquity in chemical research and the expected intensity ratio relative to SDS being higher and lower for a comparable number of negative polarity candidates. Table 1 depicts the results of these experiments. For many of these, the gas phase acidities were found from reports in the literature. To the best of our knowledge, this property has yet to be determined for some of the ions investigated herein. Thus, their predicted or experimentally determined in-solution acidity (pK_a) was correlated to our results. Although pK_a and gas phase acidities are distinctive, this correlation is justified by previous studies demonstrating that pK_a has an inverse relationship to response in the negative ESI.⁴⁷

The first anionic species to be examined were β -diketone **1** and α -triflyl ketones **2** and **3**, which had been previously synthesized by methods developed in our research group.⁴¹ α -Triflyl species are unique in that they contain one of the most powerful neutral electron withdrawing groups, $-\text{SO}_2\text{CF}_3$. This was anticipated to provide desirable results by increasing the acidity of the central methylene carbon. However, these were the worst performing of all 25 charged candidates. In conducting EMS scans over a variety of different conditions, concentrations, and samples prepared, these species could not be detected despite initial expectations of an increase in gas-phase acidity of the methylene group relative to α -triflyl esters and 3° amides. Similar results were observed when investigating other electron withdrawing groups, such as nitrile and nitro groups of ions **4** and **5**.

Table 1. Intensity ratios of ions 1–25 found relative to SDS

Ion	Structure and m/z	Intensity Relative to SDS (%)	Gas phase acidity ^a (kcal/mol) In-solution pK_a^b
1	 m/z 223.1	0	9.7 ^b (H ₂ O) 13.35 ^b (DMSO) ⁴⁸

2	 m/z 328.9	0	ca. 5 ^b (DMSO) ⁴⁸
3	 m/z 251.0	0	5.1 ^b (DMSO) ⁴⁸
4	 m/z 65.0	0	11 ^b (H ₂ O)
5	 m/z 132.0	0	5.82 ^b (H ₂ O) ¹⁰
6	 m/z 263.0	0.5 ± 0.1	18.1 ^b (DMSO) ⁴⁸
7	 m/z 295.0	2.7 ± 0.3	12.25 ^b (DMSO) ⁴⁸ 11.0 ^b (H ₂ O) ⁴⁹
8	 m/z 244.0	3.1 ± 0.4	N/A
9	 m/z 260.0	8.6 ± 0.4	N/A
10	$\text{C}_{11}\text{H}_{23}\text{O}_2^-$ m/z 199.2	8.9 ± 2.0	5.3 ^b (H ₂ O) ⁵⁰
11	 m/z 303.1	55.0 ± 2.0	6.8 ^b (H ₂ O) 6.4 ^b (DMSO) ⁵¹ (ethyl ester)
12	$\text{C}_{12}\text{H}_{25}\text{O}_2^-$ m/z 265.1	100.0 ± 0.0	N/A
13	 m/z 279.9	115.0 ± 5.0	286.5 ^{a, 52}
14	 m/z 145.0	123.0 ± 2.0	276.6 ^{a, 53}
15	 m/z 288.0	125.0 ± 2.0	294.8 ^{a, 52}
16	$\text{C}_{12}\text{H}_{25}\text{O}_2^-$ m/z 249.2	133.0 ± 7.0	1.8 ^b (H ₂ O)
17	 m/z 278.9	154.0 ± 21.0	300.6 ^{a, 52} -1 ^b (H ₂ O) 2.1 (DMSO) ⁴⁸
18	 m/z 207.0	184.0 ± 5.0	310.3 ^a 5.3 ^b (H ₂ O) ⁵⁴

19		238.0 ± 2.0	≤1 ^b (H ₂ O) ⁵⁵
	m/z 290.9		
20		293.0 ± 2.0	< 1 ^b (H ₂ O) ⁵²
	m/z 498.9		
21		304.0 ± 15.0	284.2 ^{a, 52}
	m/z 291.9		
22		307.0 ± 9.0	N/A
	m/z 391.2		
23		332.0 ± 25.0	N/A
	m/z 863.1		
24		380.0 ± 24.0	288.7 ^{a, 56}
	m/z 578.9		
25		939.0 ± 92.0	285.1 ^{a, 57}
	m/z 579.9		

To examine the effects of oxidation state of sulfur on ESI response, bis(phenylsulfonyl)methylidene (**6**) and bis(phenylsulfonyl)methylidene (**7**) were surveyed. Both failed to outperform SDS, with recorded intensity ratios of 0.54% ± 0.1% and 2.7% ± 0.3% respectively. However, the observed 5-fold difference between them follows the trend of increasing gas-phase acidity with the oxidation state of sulfur changing from sulfinyl to sulfonyl.

Following the general trend that esters are more acidic than 3° amides, α -triflyl ester **11** was expected to have an increased gas phase acidity relative to α -triflyl pyrrolidine and morpholine amides **8** and **9**. The intensity ratios of **8** and **9** were 3.1% ± 0.4% and 8.6% ± 0.4%, respectively. Compared to **8** and **9**, α -triflyl ester **11** resulted in an intensity ratio of 55.0% ± 2.0%, representing an 18- and 6-fold intensity increase respectively. Thus, these findings remarkably exemplified our initial hypothesis. The α -triflyl amides exhibited interesting results when compared to carboxyl moieties, such as lauric acid (**10**), which afforded an intensity ratio of 8.9% ± 2.0%. Thus, **8**, **9**, and **10** had comparable intensity ratios despite a hypothesized decrease in acidity of the carboxyl functional group relative to α -triflyl amides.

Despite the unfavorable results of α -triflyl ketones and amides, we found it necessary to investigate bistriflyl species in the form of carbon and nitrogen-based acids. It was hypothesized that the enhanced electron withdrawing propensity of these groups would encourage ions **13** and **17** to

outperform SDS. To our delight, the intensity ratio of ions **13** and **17** were 115.0% ± 5.0% and 154.0% ± 21.0 % respectively. From this, we could establish a noteworthy comparison. Substitution of α -CF₃ moiety for a phenyl group had no significant effect on ESI response in N-based acids, since ions **13** and **15** were separated by less than 9% difference in intensity ratio. In contrast, ion **3** was not observed, while **17** clearly outperformed SDS. Notably, ion **13** was expected to outperform **17**, given the literature values for their gas phase acidities. This prompted the investigation of the effect of counter cations on ESI response which is discussed later.

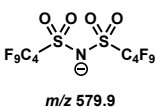
Atom linkage effects on MS performance were best illustrated by comparing the intensity ratios of the dithiane tetraoxide anion **19** to dithiazinane tetraoxide anion **21** with intensity ratios of 238.0% ± 2.0% and 304.0% ± 15.0% respectively. The improved intensity ratio of the latter may be rationalized by electronegativity differences between carbon and nitrogen but also by the increased gas-phase acidity of related C- and N-bis(sulfonyl) analogues. Overall, it was hypothesized that the increased intensity ratio of **21** was due to its extremely low gas phase acidity.

The effects of incorporating perfluoroalkyl groups on response was investigated via examining the MS performance of **16** and **20**. Predictably, there was an enhancement of signal intensity, with recorded ratios of 133.0% ± 7.0% and 293.0% ± 2.0% respectively. The increased signal intensity ratio from **16** to **20** is consistent with increased gas-phase acidity of **16** to **20**, which has been shown for the methyl- and trifluoromethyl analogues.⁵⁶ Further, **18** with an intensity ratio of 184.0% ± 5.0%, evidently did not suffer from the same effects as the undetected β -diketone **1** and outperformed **17** despite the hypothesized increased gas phase acidity of **17** relative to **18**. This enrichment encouraged further exploration of electron deficient perfluoroalkyl groups within other species.

To this end, we chose to investigate the performance of sodium bis(nonafluorobutanesulfonyl)methanide (**24** + Na⁺) and potassium bis(nonafluorobutanesulfonyl)imide (**25** + K⁺). Not only did these species outperform SDS, but ion **25** had a remarkable intensity ratio of 939.0% ± 92.0%. To further probe the MS performance of ion **25**, three truly fixed, permanently charged anions—hexafluorophosphate (**14**), tetrakis(phenyl)borate (**22**), and tetrakis(3,5-bis(trifluoromethyl)phenyl)borate (**23**)—were investigated. These non-coordinating anions are theoretically less prone to charge quenching via gas phase basicity. On that basis, it was interesting to examine how their MS performance would compare to SDS, as well as ions **24** and **25**. Validating this initial hypothesis, these anions all had highly desirable intensity ratios, but it was fascinating that MS behaviour of ion **25** remained unparalleled.

Comparisons of the intensity ratios of ions **13** and **17** as well as **19** to **21** stimulated investigations concerning the effect of different counter cations on observed signal intensities. These experiments were conducted with ion **25** since it was the best performing species, and the preparation of its different salts proved facile and inexpensive.

Table 2. Cation effects on observed MS intensity ratio

Ion	Counter cation	Intensity Relative to 12 (%)
 m/z 579.9 25	H ⁺	3195.0 ± 145.0
	Na ⁺	1616.0 ± 112.0
	NH ₄ ⁺	1450.0 ± 129.0
	K ⁺	939.0 ± 92.0

Chosen counter cations ranged from hard cations (e.g., Na⁺ and H⁺) to softer cations (e.g., K⁺ and NH₄⁺). At the outset of these experiments, it was anticipated that a hard-soft mismatch between the counter cation and **25** would provide more desirable signal intensities. The obtained results (Table 2) not only validated our initial hypothesis, but also highlighted the astounding effect of the counter cation choice has on signal intensity, with (**25** + H⁺) having the highest-recorded intensity ratio of 3195.0% ± 145.0%. It is also worth noting that although ammonium cation is softer than potassium, the increased signal intensity of (**25** + NH₄⁺) when compared to (**25** + K⁺) could be attributed to hydrogen bonding between NH₄⁺ and acetonitrile.

Results of the previously discussed intensity ratio experiments led us to conclude that ions **18-25** had the best MS performance. Although **25** proved to be unmatched amongst these species, we found it necessary to conduct solvent matrix effects experiments (Figure 1, see Supporting Information for more information). In these experiments, samples of equimolar mixtures of SDS (**12**) as well as **18-25** were analyzed in different solvent compositions.

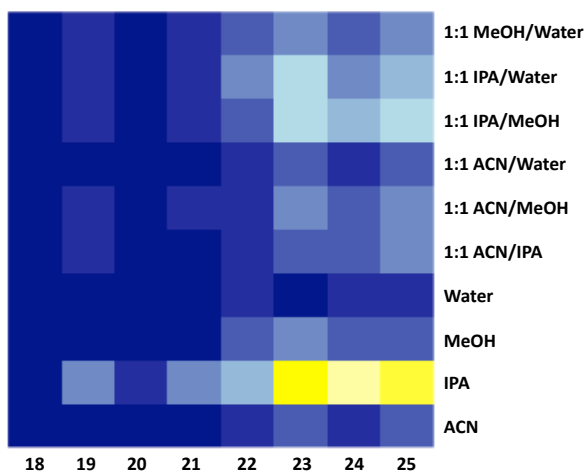


Figure 1. Heatmap depicting the intensity ratio (%) relative to SDS of ions **18-25** in different solvent compositions (see Supporting Information for Heatmap Key)

When mixtures of these ions were analyzed in neat acetonitrile (ACN), it was evident that ions **22-25** remained the top performing ions, but **18-21** and was marginally affected with the increased matrix complexity. Based on the ion evaporation model, it was expected that the intensity ratio of these ions relative to SDS would be enhanced in more

polar solvents for ions with hydrophobic characteristics. To this effect, we probed and compared MS behaviour in other pure solvents including: (1) 2-propanol (IPA); (2) methanol (MeOH); and (3) water. Comparatively, ion **18** displays increased polarity, thus, it demonstrated no significant signal enhancement. On the other hand, the MS behavior of ions **19-21** improved in IPA and diminished in MeOH and water. Interestingly, **22-25** exhibited the best intensity in IPA followed by MeOH. Overall, neat IPA appears to be the solvent of choice for improved MS behavior, and the performance of ions **18-25** was negatively impacted the most in water.

Further, as ACN, IPA, MeOH, and water are ubiquitous in isocratic and gradient elution LC-MS, we investigated all six possible 1:1 binary combinations of these solvents. Compared to ACN, ions **18-22** had no desirable improvement in signal intensity. Conversely, **23-25** showed significant signal enhancements, especially in 1:1 IPA/MeOH and 1:1 IPA/water. Thus, solvent experiments demonstrate the compatibility of these species in different LC solvent systems.

Cumulatively, cation and solvent effects experiments demonstrated that sensitivity is not merely impacted by gas-phase acidity values alone. Instead, signal intensity is influenced by a combination of factors (e.g., choice of counter cation, solvent selection and additives, in-source fragmentation, gas-phase acidity, etc.). Since ions **23** and **25** displayed highly competitive intensities, these were ideal candidates for ESI polarity comparison experiments discussed later.

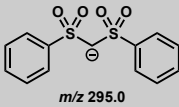
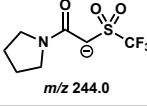
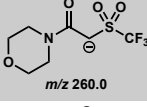
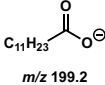
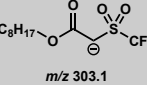
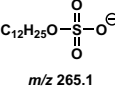
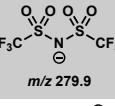
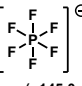
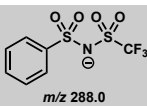
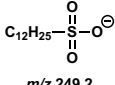
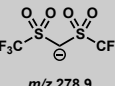
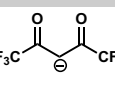
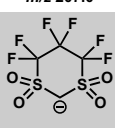
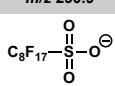
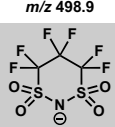
Apart from this, the MS behavior of species **1-25** was further probed by examining their precursor ion stabilities to CID by determining their SYs at a collision energy of -50 eV (Table 3). For ions **1-6**, SYs could not be determined due to the absence of their pseudomolecular ion in EMS scans.

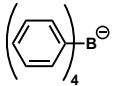
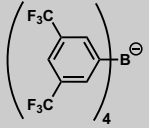
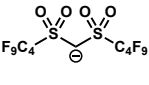

Ion **11** presented a survival yield of 1.4% ± 0.3% making it the lowest survival yield of all ions surveyed. The extremely low survival yield for ion **11** was attributed to the relative lability of the ester and triflyl moieties giving rise to a high abundance of acyl and triflyl radical fragment anions upon CID of the selected ion.

Along the same lines as **11**, **12** and **16** gave poor survival yield values at -50 eV with values of 3.2% ± 0.4% and 4.8% ± 0.5% respectively. Ion **12** proved to be quite labile to collisional activation from the formation of sulfate and sulfur trioxide radical anions upon homolytic cleavage of the carbon-oxygen bond and sulfur-oxygen single bonds attaching the sulfate moiety to the carbon backbone. Similarly, the low survival yield of ion **16** was accounted for by homolytic cleavage of the carbon-sulfur bond to generate sulfur trioxide radical as a highly abundant product ion.

Ion **18** was shown to be quite labile to CID resulting in a survival yield of 5.7% ± 0.8%. This low survival of the parent ion after collisional activation stemmed from the cleavage of the carbon-carbon bond of the acyl trifluoromethyl group.

Table 3. Survival yields of the anions 1-25 determined at a CID energy of -50 eV

Ion	Structure and m/z	Survival Yield (%)	Product Ions Observed (m/z)
7	 m/z 295.0	19.7 ± 3.3	154.8, 140.8, 79.5, 64.5
8	 m/z 244.0	11.6 ± 1.7	174.4, 132.7, 82.7, 69.1, 64.5
9	 m/z 260.0	12.2 ± 3.4	190.1, 173.1, 147.1, 104.1, 69.1, 64.1
10	 m/z 199.2	13.9 ± 1.9	180.9, 108.9
11	 m/z 303.1	1.4 ± 0.3	173.2, 147.0, 127.1, 104.3
12	 m/z 265.1	3.2 ± 0.4	97.1, 80.2
13	 m/z 279.9	14.3 ± 3.1	211.1, 147.1, 83.2, 78.2
14	 m/z 145.0	100.0 ± 0.0	N/A
15	 m/z 288.0	10.7 ± 1.9	218.7, 155.1, 91.3
16	 m/z 249.2	4.8 ± 0.5	80.2
17	 m/z 278.9	11.5 ± 1.2	210.1, 146.1, 82.4, 77.2
18	 m/z 207.0	5.7 ± 0.8	137.1, 69.2
19	 m/z 290.9	27.7 ± 1.8	207.2 (100%), 143.3, 93.3
20	 m/z 498.9	95.7 ± 0.9	419.4, 280.5, 169.2, 80.6
21	 m/z 291.9	75.8 ± 0.8	227.9, 114.1, 83.2

22	 m/z 391.2	55.3 ± 3.1	241.3, 77.3
23	 m/z 863.1	100.0 ± 0.0	N/A
24	 m/z 578.9	60.6 ± 0.4	360.7, 296.6, 78.8
25	 m/z 579.9	72.6 ± 0.8	363.5, 297.7, 144.8,

Amide containing ions **8** and **9** with survival yields of 11.6% ± 1.7% and 12.2% ± 3.4% resulted in similar survival yields in comparison to ions **13**, **15**, and **17** that gave survival yields of 14.3% ± 3.1%, 10.7% ± 1.9% and 11.5% ± 1.2% respectively. The crux of the relative instability of these ions results from the fragmentation of the labile triflyl functionality that give rise to highly abundant product ions from cleavage of the sulfur-carbon bond of the trifluoromethyl group and cleavage of the adjacent carbon-sulfur bond. Thus, it was concluded that triflyl functionalities are particularly labile via collisional activation.

In contrast to the bistriflyl ion **17**, ion **7** resulted in a higher survival yield when subjected to collisional activation with a percentage of 19.7% ± 3.3%. The product ions that were produced from collisional activation arise from similar cleavage of the carbon-sulfur bond attaching the phenyl ring to the sulfonyl moiety and the adjacent carbon-carbon bond. However, the near doubling of the survival yield of ion **7** does not make up for its poor MS signal intensity.

An additional ion of intermediate signal intensity was carboxylate ion **11** with a survival yield of 13.9% ± 1.9%. Ion **11** follows the same trend as ion **7** in that despite the increased survival yield relative to the best triflyl-containing ions, inferior MS signal intensity makes it an unsuitable fixed charge species.

Considering the survival yields of the triflyl containing ions, other perfluorinated bis(sulfonyl) ions were evaluated with modification of the perfluorinated scaffold connectivity, chain length, and electron withdrawing capacity in effort to increase survival yield upon CID. It was hypothesized that the added structural rigidity of ions **19** and **21** would increase the overall survival yield relative to the triflyl-containing ions. However, despite ion **19** having a higher survival yield of 27.7% ± 1.8%, it was almost three times less than ion **21** with a survival yield of 75.8% ± 0.8%.

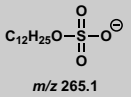
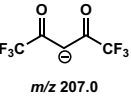
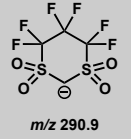
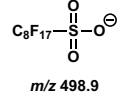
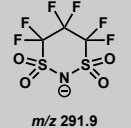
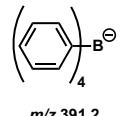
Along the same lines, the survival yield was determined for ions **24** and **25** due to the increased electron withdrawing capacity of the nonafluorobutyl chains. Similarly, to ions

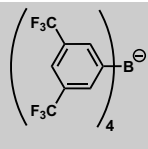
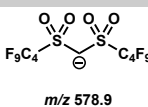
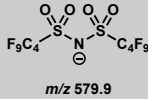
19 and **21**, ions **24** and **25** resulted in survival yields of $60.6\% \pm 0.4\%$ and $72.6\% \pm 0.8\%$ respectively indicating the ion **25** being the nitrogen acid outperformed ion **24**, the carbon acid. Additionally, despite the decreased structural rigidity of ions **24** and **25**, both still gave high survival yields comparable to ion **21**. Thus, the increased mass⁵⁸ and electron withdrawing capacity of these significantly improved survival yield as compared to the triflyl-containing ions.

Results of survival yield experiments at a collision energy of -50 eV indicated that ions **14** and **20-25** are particularly stable to collisional activation. To truly demonstrate this, further experiments were conducted at lower collision energies of -20 eV and -30 eV for ions **12** and **18-25** (Table 4). Ion **14** was excluded from this because of its inferior signal intensity ratio. Instead, we chose to analyze ion **18** since it performed considerably better in MS intensity experiments. Further, it would be beneficial to probe whether **12** and **18** would benefit from increased stability to collisional activation at lower energies.

Comparatively, ions **12** and **18** exhibited a marginal increase in stability at -20 eV, with survival yields of $100.0\% \pm 0.0\%$ and $82.1\% \pm 0.1\%$ respectively. Ion **18** did not fare well at -30 eV with a survival yield of $28.3\% \pm 0.1\%$, but **12** still boasted a higher survival yield of $68.6\% \pm 0.6\%$. Predictably, ions **21-25** remained stable to collision activation with a survival yield of $100.0\% \pm 0.0\%$.

Table 4. Survival yields of anions 12 and 18-25 determined at a CID energy of -20 eV and -30 eV

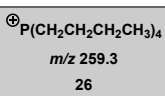
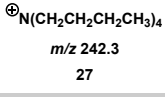
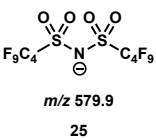
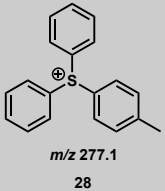
Ion	Structure and m/z	Survival Yield (%) at -20 eV	Survival Yield (%) at -30 eV
12	 m/z 265.1	100.0 ± 0.0	68.6 ± 0.6
18	 m/z 207.0	82.1 ± 0.1	28.3 ± 0.1
19	 m/z 290.9	100.0 ± 0.0	92.5 ± 0.1
20	 m/z 498.9	100.0 ± 0.0	100.0 ± 0.0
21	 m/z 291.9	100.0 ± 0.0	100.0 ± 0.0
22	 m/z 391.2	100.0 ± 0.0	100 ± 0.0

23	 m/z 863.1	100.0 ± 0.0	100.0 ± 0.0
24	 m/z 578.9	100.0 ± 0.0	100.0 ± 0.0
25	 m/z 579.9	100.0 ± 0.0	100.0 ± 0.0

To our delight, ion **25** surpassed all three of the permanently positively charged species. Relative to **28**, **25** was found to have an intensity ratio of $180.7\% \pm 13.8\%$. Literature derived reports demonstrated that phosphonium species lacking structural rigidity are typically less responsive than flexible ammonium species, like tetra-*n*-butylammonium (**27**).⁵⁹ With that premise, it was expected that ion **25** would have a higher intensity ratio relative to **27**.

We observed the contrary with **25** having an intensity ratio of $174.1\% \pm 9.1\%$ and $136.2\% \pm 5.5\%$ relative **26** and **27**, respectively. Nevertheless, negative ion **25** outperformed all 3 fixed permanent charge species. Therefore, the dogma of negative ion mode being less sensitive than the positive ion mode was successfully disproven by displaying a negatively charged functionality that outperforms some of the best and most widely used fixed charge species in the positive ion mode.

Table 5. Sensitivity comparisons between the negative and positive polarities of ESI

Negative Ion	Positive Ion	Intensity Relative to Positive Ion (%)
	 m/z 259.3 26	136.2 ± 5.5
	 m/z 242.3 27	174.1 ± 9.1
 m/z 579.9 25	 m/z 277.1 28	180.7 ± 13.8

Conclusions

In the course of this work, 25 ions were evaluated for their ESI-MS properties with respect to signal intensity relative to an internal standard of SDS and the resistance of these ions to collision-induced dissociation at -50 eV. Individually compared to SDS, tetrakis[3,5-bis(trifluoromethyl)phenyl]borate anion (**23**) and bis(nonafluoro-1-butane)sulfonimide (**25**) exhibited remarkable intensity

ratios of 332.0% ± 25.0% and 939.0% ± 92.0% respectively. Further, deviations of intensity ratio trends from gas phase acidity and pK_a values were observed. This prompted a thorough investigation of other factors that may potentially impact recorded intensity values, namely the choice of counter cation and solvent composition.

Cation effect experiments were conducted with ion **25** since it previously exhibited optimal signal intensity and preparations of its ammoniated (**25** + NH₄⁺), sodiated (**25** + Na⁺), and potassiated (**25** + K⁺) salts from its neutral form (**25** + H⁺) proved facile and inexpensive. It was observed that a hard-soft mismatch between the anion and cation significantly impacted intensity with (**25** + H⁺) boasting the overall highest-recorded ratio of 3195.0% ± 145.0%, and (**25** + Na⁺), (**25** + NH₄⁺), and (**25** + K⁺) exhibiting ratios of 1616.0% ± 112.0%, 1450.0% ± 129.0%, and 939.0% ± 92.0% respectively.

Also, ions **18-25** were chosen for further examination of solvent matrix effects on signal intensity using solvents of acetonitrile, methanol, isopropanol, water, and their respective 1:1 mixtures. It was discerned that ions **23** and **25** were of the greatest compatibility and performance in most solvent mixtures, owing to their exceptionally low proton affinities in concert with innate solvophobicity facilitating their desolvation. Overall, cation and solvent composition effects demonstrated that signal intensity in ESI is the result of a complex interplay of various factors. This ultimately reinforces the central theme of this work: the poor perception of the sensitivity of negative ion mode can be attributed to the ionization efficiency of species investigated thus far.

Finally, to challenge the notion of inherently lower sensitivity of negative ion mode when compared to the positive, the signal intensity of **25** in the negative polarity was compared to tetra-*n*-butylammonium (**26**), tetra-*n*-butyl-phosphonium (**27**), and (4-methylphenyl)diphenylsulfonium (**28**) signal intensities in the positive polarity. Ion **25** was determined to be 136.2% ± 5.5% to 180.7% ± 13.8% of the positive cation signal intensities indicating that **25**, a negative ion, outperformed the most frequently used fixed positive charge moieties. Collectively, the identification of species exhibiting desirable negative ion mode ESI-MS behaviour without the incorporation of special additives, solvents, or protocols demonstrates that negative ion mode ESI is just as sensitive as the positive mode. It is hoped that the presented findings encourage further studies into the applications of negative ion mode ESI.

ASSOCIATED CONTENT

Supporting Information

This material is available free of charge via the internet at .

AUTHOR INFORMATION

Corresponding Author

Jeffrey M. Manthorpe – Department of Chemistry and Institute of Biochemistry, Carleton University, Ottawa, ON K1S 5B6, Canada; orcid.org/0000-0002-6966-6797; Phone: +1 613-530-2600 ext. 1711; Email: jeff.manthorpe@carleton.ca

Authors

Benjamin B. Warnes – Department of Chemistry, Carleton University, Ottawa, ON K1S 5B6, Canada; <http://orcid.org/0009-0002-2024-227X>

Jasmine Chihabi – Department of Chemistry, Carleton University, Ottawa, ON K1S 5B6, Canada; <http://orcid.org/0009-0000-7019-2624>

Author Contributions

†B.B.W. and J.C. contributed equally to this work.

Funding Sources

The Natural Science and Engineering Research Council of Canada (NSERC).

Notes

The authors declare no competing financial interests.

ACKNOWLEDGMENTS

J.M.M. would like to thank the Natural Sciences and Engineering Research Council of Canada, and Carleton University for research funding. B.B.W. and J.C. gratefully acknowledge Carleton University for the support of internal scholarships the Natural Sciences and Engineering Research Council of Canada for the support of the Canadian Graduate Scholarship – Masters. J.M.M., B.B.W., and J.C. thank Prof. Dr. Hikaru Yanai and Prof. Dr. Prof. Dr. Charles McDonald for their generosity.

ABBREVIATIONS

ACN, acetonitrile; CD, chemical derivatization; CID, collision-induced dissociation; EMS; enhanced mass spectrometry scan; ESI-MS, electrospray ionization mass spectrometry; HPLC, high performance liquid chromatography; IPA, isopropanol; MS, mass spectrometry; *m/z*, mass-to-charge ratio; MeOH, methanol; pK_a, in-solution acidity; LC-MS, liquid chromatography mass spectrometry; IE, ionization efficiency, IS, ion source; PEEK, polyether ether ketone, PTFE, Polytetrafluoroethylene; S/N, signal-to-noise; SDS, sodium dodecylsulfate; SY, survival yield; MS/MS, tandem mass spectrometry; TCI, Tokyo Chemical Industry

REFERENCES

- (1) Konermann, L.; Ahadi, E.; Rodriguez, A. D.; Vahidi, S. Unraveling the Mechanism of Electrospray Ionization. *Anal. Chem.* 2013, 85 (1), 2–9. <https://doi.org/10.1021/ac302789c>.
- (2) Wani, A. H.; Udgaonkar, J. B. Mass Spectrometry Studies of Protein Folding. *Curr. Sci.* 2012, 102 (2), 245–265.
- (3) Marczak, L.; Idkowiak, J.; Tracz, J.; Stobiecki, M.; Perek, B.; Kostka-Jeziorny, K.; Tykarski, A.; Wanic-Kossowska, M.; Borowski, M.; Osuch, M.; Formanowicz, D.; Luczak, M. Mass Spectrometry-Based Lipidomics Reveals Differential Changes in the Accumulated Lipid Classes in Chronic Kidney Disease. *Metabolites* 2021, 11 (5), 275. <https://doi.org/10.3390/metabo11050275>.
- (4) Rager, J. E.; Strynar, M. J.; Liang, S.; McMahan, R. L.; Richard, A. M.; Grulke, C. M.; Wambaugh, J. F.; Isaacs, K. K.; Judson, R.; Williams, A. J.; Sibus, J. R. Linking High Resolution Mass Spectrometry Data with Exposure and Toxicity Forecasts to Advance High-Throughput Environmental Monitoring. *Environ. Int.* 2016, 88, 269–280. <https://doi.org/10.1016/j.envint.2015.12.008>.
- (5) Sun, Q.; Dong, Y.; Wen, X.; Zhang, X.; Hou, S.; Zhao, W.; Yin, D. A Review on Recent Advances in Mass Spectrometry Analysis of Harmful Contaminants in Food. *Front. Nutr.* 2023, 10, 1244459. <https://doi.org/10.3389/fnut.2023.1244459>.
- (6) Swiner, D. J.; Jackson, S.; Burris, B. J.; Badu-Tawiah, A. K. Applications of Mass Spectrometry for Clinical Diagnostics: The

- Influence of Turnaround Time. *Anal. Chem.* 2020, 92 (1), 183–202. <https://doi.org/10.1021/acs.analchem.9b04901>.
- (7) Liigand, P.; Kaupmees, K.; Kruve, A. Influence of the Amino Acid Composition on the Ionization Efficiencies of Small Peptides. *J. Mass Spectrom.* 2019, 54 (6), 481–487. <https://doi.org/10.1002/jms.4348>.
- (8) Kerwin, J. L.; Wiens, A. M.; Ericsson, L. H. Identification of Fatty Acids by Electrospray Mass Spectrometry and Tandem Mass Spectrometry. *J. Mass Spectrom.* 1996, 31 (2), 184–192. [https://doi.org/10.1002/\(SICI\)1096-9888\(199602\)31:2<184::AID-JMS283>3.0.CO;2-2](https://doi.org/10.1002/(SICI)1096-9888(199602)31:2<184::AID-JMS283>3.0.CO;2-2).
- (9) Randolph, C. E.; Blanksby, S. J.; McLuckey, S. A. Enhancing Detection and Characterization of Lipids Using Charge Manipulation in Electrospray Ionization-Tandem Mass Spectrometry. *Chem. Phys. Lipids* 2020, 232, 104970. <https://doi.org/10.1016/j.chemphyslip.2020.104970>.
- (10) Cecchi, L.; Sarfo, F. D.; Machetti, F. Isoxazoline Derivatives from Activated Primary Nitrocompounds and Tertiary Diamines. *Tetrahedron Lett.* 2005, 46 (46), 7877–7879. <https://doi.org/10.1016/j.tetlet.2005.09.110>.
- (11) Gornischeff, A.; Liigand, J.; Rebane, R. A Systematic Approach toward Comparing Electrospray Ionization Efficiencies of Derivatized and Non-Derivatized Amino Acids and Biogenic Amines. *J. Mass Spectrom.* 2018, 53 (10), 997–1004. <https://doi.org/10.1002/jms.4272>.
- (12) Straub, R. F.; Voyksner, R. D. Negative Ion Formation in Electrospray Mass Spectrometry. *J. Am. Soc. Mass Spectrom.* 1993, 4 (7), 578–587. [https://doi.org/10.1016/1044-0305\(93\)85019-T](https://doi.org/10.1016/1044-0305(93)85019-T).
- (13) Xu, C.; Doddiba, E.; Padivitage, N. L. T.; Breibach, Z. S.; Armstrong, D. W. Metal Cation Detection in Positive Ion Mode Electrospray Ionization Mass Spectrometry Using a Tetracationic Salt as a Gas-Phase Ion-Pairing Agent: Evaluation of the Effect of Chelating Agents on Detection Sensitivity. *Rapid Commun. Mass Spectrom.* 2012, 26 (24), 2885–2896. <https://doi.org/10.1002/rcm.6413>.
- (14) Liigand, P.; Kaupmees, K.; Haav, K.; Liigand, J.; Leito, I.; Girod, M.; Antoine, R.; Kruve, A. Think Negative: Finding the Best Electrospray Ionization/MS Mode for Your Analyte. *Anal. Chem.* 2017, 89 (11), 5665–5668. <https://doi.org/10.1021/acs.analchem.7b00096>.
- (15) Liu, C.; Muddiman, D. C.; Tang, K.; Smith, R. D. Improving the Microdialysis Procedure for Electrospray Ionization Mass Spectrometry of Biological Samples. *J. Mass Spectrom.* 1997, 32 (4), 425–431. [https://doi.org/10.1002/\(SICI\)1096-9888\(199704\)32:4<425::AID-JMS493>3.0.CO;2-E](https://doi.org/10.1002/(SICI)1096-9888(199704)32:4<425::AID-JMS493>3.0.CO;2-E).
- (16) Cech, N. B.; Enke, C. G. Practical Implications of Some Recent Studies in Electrospray Ionization Fundamentals. *Mass Spectrom. Rev.* 2001, 20 (6), 362–387. <https://doi.org/10.1002/mas.10008>.
- (17) Liko, I.; Hopper, J. T. S.; Allison, T. M.; Benesch, J. L. P.; Robinson, C. V. Negative Ions Enhance Survival of Membrane Protein Complexes. *J. Am. Soc. Mass Spectrom.* 2016, 27 (6), 1099–1104. <https://doi.org/10.1007/s13361-016-1381-5>.
- (18) Shields, S. W. J.; Rosales, C. A.; Roberts, J. A.; Pallister, P. J.; Wasslen, K. V.; Manthorpe, J. M.; Smith, J. C. ITrEnDi: In Situ Trimethylation Enhancement Using Diazomethane: Improved and Expanded Glycerophospholipid and Sphingolipid Analyses via a Microscale Autonomous Derivatization Platform. *Anal. Chem.* 2021, 93 (2), 1084–1091. https://doi.org/10.1021/ACS.ANALCHEM.0C04088/SUPPL_FILE/AC0C04088_SI_001.PDF.
- (19) Rosales, C. A.; Shields, S. W. J.; Aulenback, C. L. J.; Elezi, G.; Wasslen, K. V.; Pallister, P. J.; Faull, K. F.; Manthorpe, J. M.; Smith, J. C. Improved Chromatography and MS-Based Detection of Glyphosate and Aminomethylphosphonic Acid Using iTrEnDi. *J. Am. Soc. Mass Spectrom.* 2023, 34 (5), 948–957. <https://doi.org/10.1021/jasms.3c00026>.
- (20) An, N.; Zhu, Q.-F.; Wang, Y.-Z.; Xiong, C.-F.; Hu, Y.-N.; Feng, Y.-Q. Integration of Chemical Derivatization and In-Source Fragmentation Mass Spectrometry for High-Coverage Profiling of Submetabolomes. *Anal. Chem.* 2021, 93 (32), 11321–11328. <https://doi.org/10.1021/acs.analchem.1c02673>.
- (21) Unsuihuay, D.; Qiu, J.; Swaroop, S.; Nagornov, K. O.; Kozhinov, A. N.; Tsybin, Y. O.; Kuang, S.; Laskin, J. Imaging of Triglycerides in Tissues Using Nanospray Desorption Electrospray Ionization (Nano-DESI) Mass Spectrometry. *Int. J. Mass Spectrom.* 2020, 448, 116269. <https://doi.org/10.1016/j.ijms.2019.116269>.
- (22) Zaikin, V. G.; Borisov, R. S. Options of the Main Derivatization Approaches for Analytical ESI and MALDI Mass Spectrometry. <https://doi.org/10.1080/10408347.2021.1873100> 2021. <https://doi.org/10.1080/10408347.2021.1873100>.
- (23) Holden, D. D.; Pruet, J. M.; Brodbelt, J. S. Ultraviolet Photodissociation of Protonated, Fixed Charge, and Charge-Reduced Peptides. *Int. J. Mass Spectrom.* 2015, 390, 81–90. <https://doi.org/10.1016/j.ijms.2015.06.020>.
- (24) An, M.; Zou, X.; Wang, Q.; Zhao, X.; Wu, J.; Xu, L.-M.; Shen, H.-Y.; Xiao, X.; He, D.; Ji, J. High-Confidence de Novo Peptide Sequencing Using Positive Charge Derivatization and Tandem MS Spectra Merging. *Anal. Chem.* 2013, 85 (9), 4530–4537. <https://doi.org/10.1021/ac4001699>.
- (25) Lu, Y.; Zhou, X.; Stemmer, P. M.; Reid, G. E. Sulfonium Ion Derivatization, Isobaric Stable Isotope Labeling and Data Dependent CID- and ETD-MS/MS for Enhanced Phosphopeptide Quantitation, Identification and Phosphorylation Site Characterization. *J. Am. Soc. Mass Spectrom.* 2012, 23 (4), 577–593. <https://doi.org/10.1007/s13361-011-0190-0>.
- (26) Nie, S.; Fhaner, C. J.; Liu, S.; Peake, D.; Kiyonami, R.; Huang, Y.; Reid, G. E. Characterization and Multiplexed Quantification of Derivatized Aminophospholipids. *Int. J. Mass Spectrom.* 2015, 391, 71–81. <https://doi.org/10.1016/j.ijms.2015.07.002>.
- (27) Wang, S. S.; Wang, Y. J.; Zhang, J.; Sun, T. Q.; Guo, Y. L. Derivatization Strategy for Simultaneous Molecular Imaging of Phospholipids and Low-Abundance Free Fatty Acids in Thyroid Cancer Tissue Sections. *Anal. Chem.* 2019, 91 (6), 4070–4076. https://doi.org/10.1021/ACS.ANALCHEM.8B05680/ASSET/IMA_GES/LARGE/AC-2018-05680A_0006.JPEG.
- (28) Barry, S. J.; Carr, R. M.; Lane, S. J.; Leavens, W. J.; Manning, C. O.; Monté, S.; Waterhouse, I. Use of S-Pentafluorophenyl Tris(2,4,6-Trimethoxyphenyl)Phosphonium Acetate Bromide and (4-Hydrazino-4-Oxobutyl) [Tris(2,4,6-Trimethoxyphenyl)Phosphonium Bromide for the Derivatization of Alcohols, Aldehydes and Ketones for Detection by Liquid Chromatography/Electrospray Mass Spectrometry. *Rapid Commun. Mass Spectrom.* 2003, 17 (5), 484–497. <https://doi.org/10.1002/rcm.933>.
- (29) Cobice, D. F.; Livingstone, D. E. W.; Mackay, C. L.; Goodwin, R. J. A.; Smith, L. B.; Walker, B. R.; Andrew, R. Spatial Localization and Quantitation of Androgens in Mouse Testis by Mass Spectrometry Imaging. *Anal. Chem.* 2016, 88 (21), 10362–10367. <https://doi.org/10.1021/acs.analchem.6b02242>.
- (30) Woo, H.-K.; Go, E. P.; Hoang, L.; Trauger, S. A.; Bowen, B.; Siuzdak, G.; Northen, T. R. Phosphonium Labeling for Increasing Metabolomic Coverage of Neutral Lipids Using Electrospray Ionization Mass Spectrometry: Increasing Metabolomic Coverage of Neutral Lipids. *Rapid Commun. Mass Spectrom.* 2009, 23 (12), 1849–1855. <https://doi.org/10.1002/rcm.4076>.
- (31) Liao, P.-C.; Allison, J. Enhanced Detection of Peptides in Matrix-Assisted Laser Desorption/Ionization Mass Spectrometry through the Use of Charge-Localized Derivatives. *J. Mass Spectrom.* 1995, 30 (3), 511–512. <https://doi.org/10.1002/jms.1190300318>.
- (32) Nakajima, C.; Kuyama, H.; Tanaka, K. Mass Spectrometry-Based Sequencing of Protein C-Terminal Peptide Using α -Carboxyl Group-Specific Derivatization and COOH Capturing. *Anal. Biochem.* 2012, 428 (2), 167–172. <https://doi.org/10.1016/j.ab.2012.06.016>.
- (33) Setner, B.; Rudowska, M.; Kluczyk, A.; Stefanowicz, P.; Szewczuk, Z. The 5-Azoniaspiro[4.4]Nonyl Group for Improved MS Peptide Analysis: A Novel Non-Fragmenting Ionization Tag for Mass Spectrometric Sensitive Sequencing of Peptides. *Anal. Chim.*

- Acta 2017, 986, 71–81. <https://doi.org/10.1016/j.aca.2017.07.029>.
- (34) Nakajima, C.; Kuyama, H.; Nakazawa, T.; Nishimura, O. C-Terminal Sequencing of Protein by MALDI Mass Spectrometry through the Specific Derivatization of the α -Carboxyl Group with 3-Aminopropyltris-(2,4,6-Trimethoxyphenyl)Phosphonium Bromide. *Anal. Bioanal. Chem.* 2012, 404 (1), 125–132. <https://doi.org/10.1007/s00216-012-6093-5>.
- (35) Sun, D.; Meng, X.; Ren, T.; Fawcett, J. P.; Wang, H.; Gu, J. Establishment of a Charge Reversal Derivatization Strategy to Improve the Ionization Efficiency of Limaprost and Investigation of the Fragmentation Patterns of Limaprost Derivatives Via Exclusive Neutral Loss and Survival Yield Method. *J. Am. Soc. Mass Spectrom.* 2018, 29 (7), 1365–1375. <https://doi.org/10.1007/s13361-018-1924-z>.
- (36) Somasundaram, P.; Koudelka, T.; Linke, D.; Tholey, A. C-Terminal Charge-Reversal Derivatization and Parallel Use of Multiple Proteases Facilitates Identification of Protein C-Termini by C-Terminomics. *J. Proteome Res.* 2016, 15 (4), 1369–1378. <https://doi.org/10.1021/acs.jproteome.6b00146>.
- (37) Frankfater, C.; Jiang, X.; Hsu, F.-F. Characterization of Long-Chain Fatty Acid as N-(4-Aminomethylphenyl) Pyridinium Derivative by MALDI LIFT-TOF/TOF Mass Spectrometry. *J. Am. Soc. Mass Spectrom.* 2018, 29 (8), 1688–1699. <https://doi.org/10.1007/s13361-018-1993-z>.
- (38) Ahn, Y. H.; Yoo, J. S. Malononitrile as a New Derivatizing Reagent for High-Sensitivity Analysis of Oligosaccharides by Electrospray Ionization Mass Spectrometry. *Rapid Commun. Mass Spectrom.* 1998, 12 (24), 2011–2015. [https://doi.org/10.1002/\(SICI\)1097-0231\(19981230\)12:24<2011::AID-RCM429>3.0.CO;2-R](https://doi.org/10.1002/(SICI)1097-0231(19981230)12:24<2011::AID-RCM429>3.0.CO;2-R).
- (39) Ma, S.; Chen, F.; Zhang, M.; Yuan, H.; Ouyang, G.; Zhao, W.; Zhang, S.; Zhao, Y. Carboxyl-Based CPMP Tag for Ultrasensitive Analysis of Disaccharides by Negative Tandem Mass Spectrometry. *Anal. Chem.* 2022, 94 (27), 9557–9563. <https://doi.org/10.1021/acs.analchem.2c00287>.
- (40) Alexandridou, A.; Schorr, P.; Volmer, D. A. Comparing Derivatization Reagents for Quantitative LC-MS/MS Analysis of a Variety of Vitamin D Metabolites. *Anal. Bioanal. Chem.* 2023, 415 (19), 4689–4701. <https://doi.org/10.1007/s00216-023-04753-0>.
- (41) Kong, H. I.; Crichton, J. E.; Manthorpe, J. M. Stereoselective Synthesis of Ambiphilic Alkenes via Regioselective Methylation of α -Trifluoromethanesulfonyl Carbonyl Compounds with Trimethylsilyldiazomethane. *Tetrahedron Lett.* 2011, 52 (29), 3714–3717. <https://doi.org/10.1016/j.tetlet.2011.05.015>.
- (42) Jarvis, B. B.; Fried, H. E. Chlorination of Disulfoxides. *J. Org. Chem.* 1975, 40 (9), 1278–1280. <https://doi.org/10.1021/jo00897a021>.
- (43) Sankar, U.; Mahalakshmi, S.; Balasubramanian, K. K. A One-Pot Stereoselective Synthesis of Electron-Deficient 4-Substituted (E,E)-1-Arylsulfonylbuta-1,3-Dienes and Their Chemoselective [3+2] Cycloaddition with Azomethine Ylides – A Simple Synthesis of 1,3,4-Trisubstituted Pyrrolidines and Pyrroles. *Synlett* 2013, 24 (12), 1533–1540. <https://doi.org/10.1055/s-0033-1339181>.
- (44) Kong, H. I.; Gill, M. A.; Hrdina, A. H.; Crichton, J. E.; Manthorpe, J. M. Reactivity of α -Trifluoromethanesulfonyl Esters, Amides and Ketones: Decarboxylative Allylation, Methylation, and Enol Formation. *J. Fluor. Chem.* 2013, 153, 151–161. <https://doi.org/10.1016/j.jfluchem.2013.03.020>.
- (45) Padilla, M. S.; Bertz, C.; Berdusco, N.; Mecozzi, S. Expanding the Structural Diversity of Hydrophobic Ionic Liquids: Physicochemical Properties and Toxicity of Gemini Ionic Liquids. *Green Chem.* 2021, 23 (12), 4375–4385. <https://doi.org/10.1039/D1GC00742D>.
- (46) Barrett, A. G. M.; Bouloc, N.; Braddock, D. C.; Catterick, D.; Chadwick, D.; White, A. J. P.; Williams, D. J. Synthesis of Some Ytterbium(III) Tris-(Perfluoroalkylsulfonyl)Methides. 2002.
- (47) Henriksen, T.; Juhler, R. K.; Svensmark, B.; Cech, N. B. The Relative Influences of Acidity and Polarity on Responsiveness of Small Organic Molecules to Analysis with Negative Ion Electrospray Ionization Mass Spectrometry (ESI-MS). *J. Am. Soc. Mass Spectrom.* 2005, 16 (4), 446–455. <https://doi.org/10.1016/j.jasms.2004.11.021>.
- (48) Bordwell, F. G. Equilibrium Acidities in Dimethyl Sulfoxide Solution. *Acc. Chem. Res.* 1988, 21 (12), 456–463. <https://doi.org/10.1021/ar00156a004>.
- (49) Hibbert, F. Effect of a Phenyl Substituent on the Acidity and Rate of Ionisation of Disulphonyl-Activated Carbon Acids. *J. Chem. Soc. Perkin Trans. 2* 1978, No. 11, 1171–1173. <https://doi.org/10.1039/P29780001171>.
- (50) Sebők, Á.; Vasanits-Zsigrai, A.; Helenkár, A.; Záray, Gy.; Molnár-Perl, I. Multiresidue Analysis of Pollutants as Their Trimethylsilyl Derivatives, by Gas Chromatography–Mass Spectrometry. *J. Chromatogr. A* 2009, 1216 (12), 2288–2301. <https://doi.org/10.1016/j.chroma.2009.01.056>.
- (51) Goumont, R.; Magnier, E.; Kizilian, E.; Terrier, F. Acidity Inversions of α -NO₂ and α -SO₂CF₃ Activated Carbon Acids as a Result of Contrasting Solvent Effects on Transfer from Water to Dimethyl Sulfoxide Solutions. *J. Org. Chem.* 2003, 68 (17), 6566–6570. <https://doi.org/10.1021/jo034244a>.
- (52) Leito, I.; Raamat, E.; Kütt, A.; Saame, J.; Kipper, K.; Koppel, I. A.; Koppel, I.; Zhang, M.; Mishima, M.; Yagupolskii, L. M.; Garlyayuskayte, R. Yu.; Filatov, A. A. Revision of the Gas-Phase Acidity Scale below 300 Kcal Mol⁻¹. *J. Phys. Chem. A* 2009, 113 (29), 8421–8424. <https://doi.org/10.1021/jp903780k>.
- (53) Koppel, I. A.; Burk, P.; Koppel, I.; Leito, I.; Sonoda, T.; Mishima, M. Gas-Phase Acidities of Some Neutral Brønsted Superacids: A DFT and Ab Initio Study. *J. Am. Chem. Soc.* 2000, 122 (21), 5114–5124. <https://doi.org/10.1021/ja0000753>.
- (54) Jones, J. R.; Patel, S. P. Anomalous Brønsted Relation for β -Diketones. *J. Am. Chem. Soc.* 1974, 96 (2), 574–575. <https://doi.org/10.1021/ja00809a039>.
- (55) Zhu, S.; Xu, G.; Qin, C.; Yong, X.; Qianli, C.; DesMarteau, D. D. Chemical Transformation of Bis((Perfluoroalkyl)Sulfonyl)Methanes and 1,1,3,3-Tetraoxopolyfluoro-1,3-Dithiaycloalkanes. *Heteroat. Chem.* 1999, 10 (2), 147–151. [https://doi.org/10.1002/\(SICI\)1098-1071\(1999\)10:2<147::AID-HC8>3.0.CO;2-2](https://doi.org/10.1002/(SICI)1098-1071(1999)10:2<147::AID-HC8>3.0.CO;2-2).
- (56) Koppel, I. A.; Taft, R. W.; Anvia, F.; Zhu, S.-Z.; Hu, L.-Q.; Sung, K.-S.; DesMarteau, D. D.; Yagupolskii, L. M.; Yagupolskii, Y. L. The Gas-Phase Acidities of Very Strong Neutral Brønsted Acids. *J. Am. Chem. Soc.* 1994, 116 (7), 3047–3057. <https://doi.org/10.1021/ja00086a038>.
- (57) Zhang, M.; Sonoda, T.; Mishima, M.; Honda, T.; Leito, I.; Koppel, I. A.; Bonrath, W.; Netscher, T. Gas-Phase Acidity of Bis((Perfluoroalkyl)Sulfonyl)Imides. Effects of the Perfluoroalkyl Group on the Acidity. *J. Phys. Org. Chem.* 2014, 27 (8), 676–679. <https://doi.org/10.1002/poc.3317>.
- (58) Shukla, A. K.; Futrell, J. H. Collisional Activation and Dissociation of Polyatomic Ions. *Mass Spectrom. Rev.* 1993, 12 (4), 211–255. <https://doi.org/10.1002/mas.1280120402>.
- (59) Omari, I.; Randhawa, P.; Randhawa, J.; Yu, J.; McIndoe, J. S. Structure, Anion, and Solvent Effects on Cation Response in ESI-MS. *J. Am. Soc. Mass Spectrom.* 2019, 30 (9), 1750–1757. <https://doi.org/10.1007/s13361-019-02252-0>.

To format double-column figures, schemes, charts, and tables, use the following instructions:

Place the insertion point where you want to change the number of columns

From the **Insert** menu, choose **Break**

Under **Sections**, choose **Continuous**

Make sure the insertion point is in the new section. From the **Format** menu, choose **Columns**

In the **Number of Columns** box, type **1**

Choose the **OK** button

Now your page is set up so that figures, schemes, charts, and tables can span two columns. These must appear at the top of the page. Be sure to add another section break after the table and change it back to two columns with a spacing of 0.33 in.

Table 1. Example of a Double-Column Table

Column 1	Column 2	Column 3	Column 4	Column 5	Column 6	Column 7	Column 8

Authors are required to submit a graphic entry for the Table of Contents (TOC) that, in conjunction with the manuscript title, should give the reader a representative idea of one of the following: A key structure, reaction, equation, concept, or theorem, etc., that is discussed in the manuscript. Consult the journal's Instructions for Authors for TOC graphic specifications.

Insert Table of Contents artwork here
